

Generating entangled polaritonic condensates by pumping with entangled pairs of photons

N.A. Asriyan,^{1,2,*} A.A. Elistratov,¹ and A.V. Kavokin^{3,4,5}

¹*N.L. Dukhov Research Institute of Automatics (VNIIA), Moscow 127030, Russia*

²*Complex Systems and Statistical Mechanics, Department of Physics and Materials Science, University of Luxembourg, 30 Avenue des Hauts-Fourneaux, L-4362 Esch-sur-Alzette, Luxembourg*

³*Russian Quantum Center, Skolkovo, Moscow 143025, Russia*

⁴*St. Petersburg State University, 7/9, University Embankment, St. Petersburg 199034, Russia*

⁵*School of Science, Westlake University, 18 Shilongsham Road, Hangzhou, 310024, Zhejiang Province, China*

We investigate the steady state of two single-mode uniform spatially separated polaritonic condensates exposed to resonant pumping with entangled pairs of photons. We demonstrate the principal possibility of driving the system to an entangled state despite its exposure to noises arising from the excitonic reservoir and photon leakage through the microcavity mirrors. Estimates are provided for the flux of entangled particles required to drive the system into a steady state that violates the partial-transpose criterion for entanglement. Furthermore, we trace the evolution of the system after a sudden disappearance of the entangled pumping. Our analysis provides estimates for the entanglement lifetime in a system of two exciton-polariton condensates.

PACS numbers:

I. INTRODUCTION

Entanglement is one of the most remarkable quantum phenomena on the microscopic level. Still, its observation and manipulation at the macroscopic level remain challenging. Recent advances in experiments with cold atomic gases proved that Bose-Einstein condensates are decent candidates for this purpose. Initially, it was demonstrated that distinct spatial modes of the same condensates can exhibit quantum correlations [1] and then, finally, an entangled state of two macroscopic condensates was achieved[2].

When it comes to excitonic polaritons, there is still much more to do to obtain an experimental demonstration of macroscopic entanglement. Recent theoretical work sheds light on possible research directions. In particular, experimental setups are proposed that are potentially suitable for the demonstration of entanglement between the modes of the same condensate [3] with different polarizations, as well as for the detection of entanglement with spatially separated condensates [4]. However, only recently has it been experimentally demonstrated that it is possible to entangle single polaritons [5] with photons. Entangling massive clouds of condensed polaritons still presents a challenge that has yet to be overcome.

Despite the fundamental importance of achieving entanglement with exciton-polariton condensates, there are also applicational benefits because of the possible contribution to modern quantum technological advances [6]. One of the key features of that physical platform that is suitable for being used as a component for a qubit is the robustness of entanglement with respect to

the environmental noise. With superconducting qubits, semiconductor-based ones, and qubits based on trapped ions, the reduced temperature is the key to provide the desired robustness. Given the low particle mass and, consequently, the high temperature of preservation of collective quantum behavior, exciton-polaritons might pose less strict conditions on the temperature for entanglement preservation. Several proposals have been made on the way polaritonic conjugates can be used to create qubits [7, 8].

In general, the challenge to demonstrate macroscopic entanglement of two clouds is significant because of the highly non-equilibrium nature of the polaritonic system, which elevates the level of thermal and quantum noises. In this paper, we analyze the possibility of entanglement of polariton condensates from the quantum optical perspective. Aiming at a proof-of-principle demonstration, we resort to a brute-force method: directly injecting already entangled particles from an external source, *i.e.* we describe coupled OPO's exposed to noisy environment. This setup is a simple natural candidate for analyzing the robustness of quantum entanglement with respect to environmental noise and addressing the question of reservoir engineering (see, *e.g.* [9]).

Our goal is to find conditions under which the condensates will be entangled and to estimate the lifetime of entanglement in the noisy environment of pump and decay reservoirs. In the next section, we describe a model of the setup under consideration. Then, in Section III, follows an analysis of the stationary state of two condensates above the condensation threshold. The main results of the paper are reported in Section IV, where we derive, in general form, sufficient conditions on the intensity of two-photon entangled pumping that lead to an entangled state of the condensates. These results are followed by an estimate of the entanglement lifetime in Section V and a discussion of the implications of the results in Section

*Electronic address: norair.asriian@uni.lu

VI.

II. MODEL

The schematic of the model we use is shown in Fig. 1:

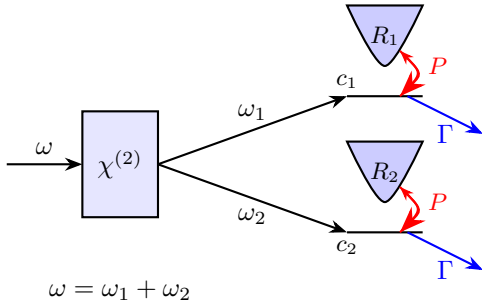


Figure 1: The schematic of a Gedankenexperiment where two exciton-polariton condensate modes (c_1 and c_2) are pumped by a source of entangled photons and coupled to independent incoherent exciton reservoirs (R_1 and R_2) that replenish polariton modes by stimulated scattering.

Two spatially separated condensates, which we describe by the two bosonic modes c_1 and c_2 , are resonantly pumped by entangled photon pairs coming from a nonlinear medium (with, *e.g.*, quadratic nonlinearity $\chi^{(2)}$) pumped by a laser with frequency ω .

To analyze such a system, we use the standard Hamiltonian of the OPO model of the form [10, 11]:

$$H(t) = \hbar\omega_1 \hat{\psi}_1^\dagger(t) \hat{\psi}_1(t) + \hbar\omega_2 \hat{\psi}_2^\dagger(t) \hat{\psi}_2(t) - \hbar\chi \left[\hat{\psi}_1^\dagger(t) \hat{\psi}_2^\dagger(t) e^{-i\omega t} + \hat{\psi}_1(t) \hat{\psi}_2(t) e^{i\omega t} \right] \quad (1)$$

with ω_1 and ω_2 being the frequencies of the signal and idler modes (which are also the frequencies of the condensate modes) and $\omega = \omega_1 + \omega_2$ due to energy conservation. Here $\hat{\psi}_{1/2}$ are the Heisenberg picture photon annihilation operators for the modes $c_{1/2}$ and χ set the intensity of pumping with entangled photonic pairs.

Hereafter, we set $\hbar = 1$. In the coherent state representation, the dynamics of the system is given by the following equation $j \in \{1, 2\}$:

$$id_t \psi_j = \omega_j \psi_j - \chi \bar{\psi}_{3-j} e^{-i\omega t}. \quad (2)$$

Assuming that the two modes are represented by identical polariton condensates coupled to their respective independent (*e.g.* spatially separated) exciton reservoirs R_1 and R_2 , we consider evolution equations of the following type:

$$id_t \psi_j = \left[\omega_j \psi_j + \frac{i}{2} (P[|\psi_j|^2] - \Gamma[|\psi|^2]) \psi_j - \chi \bar{\psi}_{3-j} e^{-i\omega t} \right] dt + \sqrt{\frac{1}{4} (Q[|\psi_j|^2] + \Gamma[|\psi|^2])} d\mathbf{W}_j. \quad (3)$$

Here, $d\mathbf{W}d\mathbf{W}^* = 2dt$, $P(|\psi|^2)$ and $\Gamma(|\psi|^2)$ represent pumping of polariton modes by stimulated scattering from the excitonic reservoir and leakage of polaritons out of the microcavity due to photon tunneling through the mirrors, respectively. The corresponding noise term components are given by $Q(|\psi|^2)$ and $\Gamma(|\psi|^2)$, respectively.

Equations of this type are usually derived in the framework of the truncated Wigner approximation starting from the master equation [12] or the Schwinger-Keldysh technique [13, 14] after adiabatically excluding the excitonic reservoir. These derivations imply a specific relation between the drift and diffusion terms. That is, if the pump drift term is a combination of inflow (to the condensate) and backflow (to the reservoir) rates $P[|\psi_j|^2] = R_{\text{in}}[|\psi_j|^2] - R_{\text{back}}[|\psi_j|^2]$, the diffusion term can be written as follows:

$$Q[|\psi_j|^2] = R_{\text{in}}[|\psi_j|^2] + R_{\text{back}}[|\psi_j|^2]. \quad (4)$$

For an equilibrated reservoir at temperature T_R with chemical potential μ_R , this expression transforms to the fluctuation-dissipation relation

$$Q[|\psi_j|^2] = \coth\left(\frac{E - \mu_R}{2kT_R}\right) P[|\psi_j|^2] = \eta P[|\psi_j|^2]. \quad (5)$$

For exciton-polariton condensates, the energy E corresponds to the separation between the lower polariton mode and the exciton resonance frequency, as demonstrated below. It depends on the Rabi splitting Ω and exciton-photon detuning Δ_0 in the following way:

$$E = \frac{\Delta_0}{2} - \sqrt{\left(\frac{\Delta_0}{2}\right)^2 + \Omega^2}, \quad (6)$$

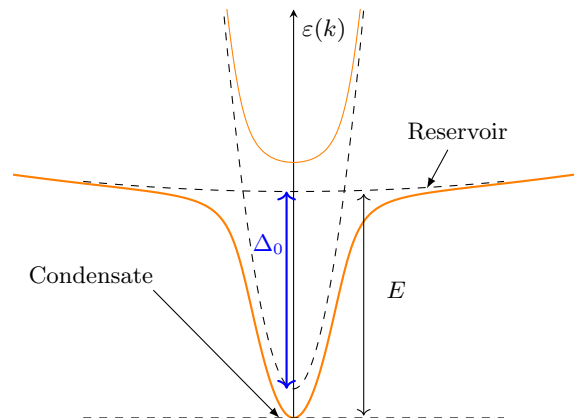


Figure 2: Dispersion curves $\varepsilon(k)$ for the lower and upper polariton modes (orange lines). For the lower polariton branch, the energy offset E between the condensate and the reservoir is indicated.

When it comes to photon leakage, it is reasonable to consider no backflow, that is why the noise variation term appears to be the same as the one for the coherent flow

in (3). We emphasize that both terms are chosen to adequately reproduce zero-point fluctuations $\langle |\psi_j|^2 \rangle = 1/2$ in the absence of any pumping.

To keep things as general as possible, we have not yet specified the exact form of the gain saturation function $P[|\psi_j|^2]$ and assume that the decay term $\Gamma[|\psi_j|^2]$ may also be saturable (but without any backflow, as is the case for photon leakage through the microcavity mirrors).

III. PROPERTIES OF THE STATIONARY STATE OF TWO ENTANGLED CONDENSATES

We will use the coordinate-momentum quadratures

$$\begin{aligned} x_j &= \frac{\psi_j e^{i\omega_j t} + \bar{\psi}_j e^{-i\omega_j t}}{2}, \\ p_j &= \frac{\psi_j e^{i\omega_j t} - \bar{\psi}_j e^{-i\omega_j t}}{2i} \end{aligned} \quad (7)$$

to represent the drift terms as sliding down a potential:

$$\begin{cases} dx_j &= -\partial_{x_j} V dt + \sqrt{\frac{1}{4} [\eta P[\rho_j] + \Gamma[\rho_j]]} dW_{xj}, \\ dp_j &= -\partial_{p_j} V dt + \sqrt{\frac{1}{4} [\eta P[\rho_j] + \Gamma[\rho_j]]} dW_{pj}. \end{cases} \quad (8)$$

with independent Wiener increments dW_{xj} and dW_{pj} . Here, we introduce

$$V(x_1, p_1, x_2, p_2) = \frac{G[\rho_1] + G[\rho_2]}{4} - \chi(p_2 x_1 + x_2 p_1) \quad (9)$$

and imply $d_\rho G[\rho] = \Gamma[\rho] - P[\rho]$ with $\rho_j = x_j^2 + p_j^2$.

Hereafter we restrict ourselves to the states with high mean occupations $\langle \rho_j \rangle \gg 1$ of the condensate modes. This allows us to treat the noise variance terms as constants. With that assumption, the stationary Wigner distribution may be explicitly derived (see [15]):

$$W(x_1, p_1, x_2, p_2) \sim \exp\left(-\frac{2V(x_1, p_1, x_2, p_2)}{\frac{1}{4}(\eta P[\langle \rho_j \rangle] + \Gamma[\langle \rho_j \rangle])}\right). \quad (10)$$

Note that the integration constant in the definition of $G[\rho]$ is fixed by normalizing the Wigner function. And due to the symmetry of the problem, $\langle \rho_1 \rangle = \langle \rho_2 \rangle$.

Note that without a flux of entangled pairs, $\chi = 0$, the distribution factorizes:

$$W(x_1, p_1, x_2, p_2) = W^{(1)}(x_1, p_1) W^{(1)}(x_2, p_2) \quad (11)$$

with

$$W^{(1)}(x_i, p_i) \sim \exp\left(-\frac{G[x_i^2 + p_i^2]}{\frac{1}{2}(\eta P[\langle x_i^2 + p_i^2 \rangle] + \Gamma[\langle x_i^2 + p_i^2 \rangle])}\right). \quad (12)$$

Above the condensation threshold $G[\rho]$ is characterized by a well-defined minimum that leads to independent ring-shaped distributions with reduced intensity correlations and a uniform phase distribution. It is a typical stationary state for 2D symmetry-broken systems, such as *e.g.* the single-mode laser [16] and atomic Bose-Einstein condensates [17]. In terms of amplitude fluctuation statistics, they are barely distinguishable from coherent states.

In both states (10) and (11) the marginal distributions in the (x_j, p_j) planes are qualitatively the same. However, the quadratures (x_1, p_2) and (x_2, p_1) are squeezed in the state (10) as schematically demonstrated in Figure 3.

We now utilize the Madelung transformation $x_j = \sqrt{\rho_j} \cos(\theta_j)$, $p_j = \sqrt{\rho_j} \sin(\theta_j)$ to express the potential as follows:

$$V(\rho, \theta_+) = \frac{1}{4} (G(\rho_1) + G(\rho_2)) - \chi \sqrt{\rho_1 \rho_2} \sin(\theta_+) \quad (13)$$

with $\theta_+ = \theta_1 + \theta_2$. The minimum of this potential is given by $\rho_1 = \rho_2 = \rho_m$, $\theta_1 + \theta_2 = \pi/2$ with

$$P[\rho_m] + 2\chi = \Gamma[\rho_m]. \quad (14)$$

In the weak-noise limit, *i.e.*, $\rho_m \gg \sqrt{\text{Var}(\rho_j)}$, we may use a Gaussian expansion for the potential (13), substitute it into the stationary Wigner function (10) and integrate over the phase difference $\theta_- = \theta_1 - \theta_2$:

$$W(\rho_1, \rho_2, \theta_+) = \mathcal{N} \exp\left[-\frac{1}{2} (\rho_1 - \rho_m \quad \rho_2 - \rho_m) \begin{pmatrix} C_{11} & C_{12} \\ C_{12} & C_{22} \end{pmatrix}^{-1} \begin{pmatrix} \rho_1 - \rho_m \\ \rho_2 - \rho_m \end{pmatrix} - \frac{1}{2C_\theta} \left(\theta_+ - \frac{\pi}{2}\right)^2\right]. \quad (15)$$

Here

$$C = \langle \delta \rho_j^2 \rangle = \frac{((1+\eta)\Gamma[\rho_m] - 2\eta\chi)(G'[\rho_m]\rho_m + \chi)}{2G'[\rho_m](G'[\rho_m]\rho_m + 2\chi)}, \quad (16)$$

$$C_{12} = \langle \delta \rho_1 \delta \rho_2 \rangle = \frac{(1+\eta)\Gamma[\rho_m] - 2\eta\chi}{2G'[\rho_m](G'[\rho_m]\rho_m + 2\chi)} \chi, \quad (17)$$

$$C_\theta = \langle \delta \theta^2 \rangle = \frac{(1+\eta)\Gamma[\rho_m] - 2\eta\chi}{8\chi\rho_m}. \quad (18)$$

When transforming back to quadratures, one can derive the following expression for the covariance matrix σ

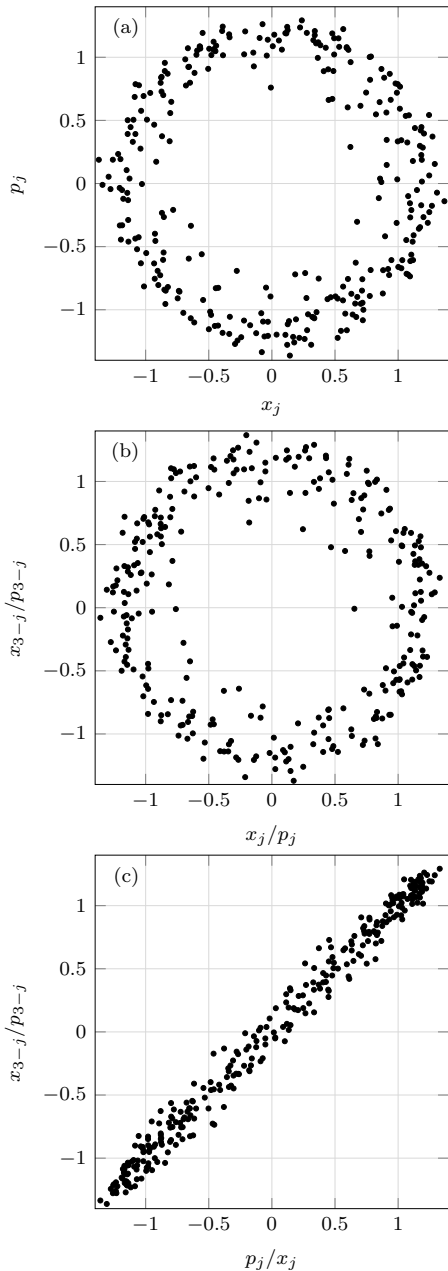


Figure 3: Wigner quasiprobability distribution illustrated for the state of type (10). The marginal distributions for (a) $p_j(x_j)$; (b) $x_j(x_{3-j})$ (for $p_j(p_{3-j})$ it looks the same); (c) $x_j(p_{3-j})$ (for $p_j(x_{3-j})$ it looks the same); are demonstrated. The Hamiltonian (1) generates squeezing in quadratures $x_j - p_{3-j}$, which results in deformation of the distributions in panel (c). These illustrative pictures are generated by simulating stochastic evolution governed by (8) with the simplest quadratic model for $G[\rho] = 2\rho - \rho^2$, $\eta = 1$, $\chi = 0.4$.

(see Appendix A):

$$\sigma = \begin{pmatrix} \langle \Delta x_1^2 \rangle & \langle \Delta x_1 \Delta p_1 \rangle & \langle \Delta x_1 \Delta x_2 \rangle & \langle \Delta x_1 \Delta p_2 \rangle \\ \langle \Delta p_1 \Delta x_1 \rangle & \langle \Delta p_1^2 \rangle & \langle \Delta p_1 \Delta x_2 \rangle & \langle \Delta p_1 \Delta p_2 \rangle \\ \langle \Delta x_2 \Delta x_1 \rangle & \langle \Delta x_2 \Delta p_1 \rangle & \langle \Delta x_2^2 \rangle & \langle \Delta x_2 \Delta p_2 \rangle \\ \langle \Delta p_2 \Delta x_1 \rangle & \langle \Delta p_2 \Delta p_1 \rangle & \langle \Delta p_2 \Delta x_2 \rangle & \langle \Delta p_2^2 \rangle \end{pmatrix} \\ = \frac{\rho_m}{2} \begin{pmatrix} 1 & 0 & 0 & \xi \\ 0 & 1 & \xi & 0 \\ 0 & \xi & 1 & 0 \\ \xi & 0 & 0 & 1 \end{pmatrix}, \quad (19)$$

where

$$\Delta x_j = x_j - \langle x_j \rangle, \\ \Delta p_j = p_j - \langle p_j \rangle$$

and

$$\xi = 1 - \frac{C - C_{12}}{4\rho_m^2} - \frac{C_\theta}{2}$$

is the effective squeezing degree of the stationary state. It is helpful to see how the reduced values of the variance in θ_+ and the difference $C - C_{12}$ lead to the squeezing effect shown in Figure 3 (c). For example, we may rotate the coordinate axes in the (x_1, p_2) plane:

$$q_\pm = \frac{x_1 \pm p_2}{\sqrt{2}}. \quad (20)$$

The variance ratio K along the two axes may serve to quantify the distribution anisotropy. As shown in details in Appendix A, we derive:

$$K = \frac{\langle q_-^2 \rangle}{\langle q_+^2 \rangle} = \frac{\frac{1}{2} \left[\frac{C - C_{12}}{4\rho_m^2} + \frac{C_\theta}{2} \right]}{1 + \frac{1}{2} \left[\frac{C - C_{12}}{4\rho_m^2} + \frac{C_\theta}{2} \right]} = \frac{1 - \zeta}{1 + \zeta}. \quad (21)$$

IV. A TEST FOR ENTANGLEMENT

The stationary state (13) (and even (15)) of condensates exposed to external pumping by entangled photon pairs is a highly non-Gaussian state (see the discussion on the degree of non-Gaussianity of ring-shaped states of the type we have here in [18]). That is why we do not have an entanglement measure to choose from, except the weak Peres-Horedecki PPT criterion in the form of a necessary condition for separability. Having derived the correlation matrix, we may utilize the adaptation of the PPT criteria for continuous variable states by R. Simon [19]. Having identified the blocks of the covariance matrix:

$$2\sigma = \begin{pmatrix} A & C \\ C^T & B \end{pmatrix}, \quad (22)$$

we should check the following inequality

$$F_{\text{PT}} = \det A \det B + \left(\frac{1}{4} - |\det C| \right)^2 - \text{tr}(AJCJBJC^T J) \\ - \frac{1}{4} (\det A + \det B) < 0 \quad (23)$$

as a sufficient (yet not necessary) condition for the quantum entanglement. Here

$$J = \begin{pmatrix} 0 & 1 \\ -1 & 0 \end{pmatrix}.$$

The factor of 2 on the left-hand side of (22) is due to the additional factor of $\sqrt{2}$ in (7) as compared to the definitions of canonical coordinate and momentum.

We divide the matrix (19) into 4 blocks and calculate the function f_{PT} . For the PPT conditions for entanglement to be satisfied, the squeezing of the state should eventually exceed a threshold value

$$\xi > 1 - \frac{1}{2\rho_m}. \quad (24)$$

Careful inspection of (16)-(18) shows that ξ can be expressed as a function of only two combinations of variables. The first is the relative entangled pumping strength with respect to the decay rate:

$$\zeta = \frac{2\chi}{\Gamma[\rho_m]}. \quad (25)$$

The second is some kind of "flux elasticity" with respect to changes in the condensate density:

$$\kappa = \frac{G'[\rho_m]\rho_m}{\Gamma[\rho_m]}. \quad (26)$$

Note that $\kappa > 0$ is a necessary condition for the stability of the condensate. The function $\kappa(\zeta)$ describes the response of incoherent reservoirs to the shift in condensate occupation caused by parametric pumping.

The condition (24) for the buildup of the entanglement can be expressed as

$$2(2 + \eta)\zeta^2 + \{(4 + \eta)\kappa(\zeta) - 2(1 + \eta)\}\zeta - (1 + \eta)\kappa(\zeta) > 0,$$

that allows finding an explicit solution for the critical value

$$\zeta_{\text{crit}} = \frac{2\eta + \sqrt{4(\eta + 1)^2 + (\eta + 4)^2\kappa^2(\zeta_{\text{crit}}) + 4\eta(\eta + 1)\kappa(\zeta_{\text{crit}})} - (\eta + 4)\kappa(\zeta_{\text{crit}}) + 2}{4(\eta + 2)}. \quad (27)$$

Clearly, the lowest critical value ζ_{crit} corresponds to the absence of backflow from the excitonic reservoir ($\eta = 1$):

$$\zeta_{\text{crit}}^{\eta=1} = \frac{1}{12} \left(\sqrt{25\kappa^2 + 8\kappa + 16 - 5\kappa + 4} \right) \in \left[\frac{2}{5}; \frac{2}{3} \right]. \quad (28)$$

The entanglement region defined by $\zeta > \zeta_{\text{crit}}^{\eta=1}$ is shown by a green area in Figure 4 which is confined with lines $\zeta_{\text{crit}}(\kappa)$ corresponding to the different values of the reservoir temperature effectively accounted for by $\eta > 1$, see (5).

The very existence of the region above ζ_{crit} is an important result of this work. This means that, even in the highly non-equilibrium system such as the polaritonic one, the fundamental fluctuation-dissipation relations do not prevent the condensates from being entangled at sufficiently high χ .

Typically for polaritons, the decay rate is mainly due to photon leakage and is weakly dependent on the density of the condensate $\Gamma \approx \text{const}$. Thus, the exact values of ζ_{crit} depend on the saturation model used to describe the flow of particles from the excitonic reservoir. We will consider two of them, which are the most frequently utilized in the literature. The first is the two-component

model proposed in Ref. [12]:

$$\begin{cases} i\hbar\dot{\psi} = \left\{ -\frac{\hbar^2\nabla^2}{2m} + \frac{i}{2} [R(n_R) - \gamma] + g|\psi|^2 + 2\tilde{g}n_R \right\} \psi + \xi(\mathbf{r}, t), \\ \dot{n}_R = P - \gamma n_R - R(n_R) |\psi(\mathbf{r})|^2 + D\nabla^2 n_R. \end{cases} \quad (29)$$

with linear $R(n_R) = Rn_R$.

For a single-mode uniform condensate, after adiabatically excluding the reservoir, we end up with the following nonlinear expression for the saturation term of (3):

$$P_{\text{nl}}[\rho] = \frac{PR}{\gamma_R + R\rho}. \quad (30)$$

The second model is just a simple linear saturation (as used first in Ref. [20]):

$$P_{\text{lin}}[\rho] = P_0 - \alpha\rho. \quad (31)$$

Notably, for both models, the function $\zeta(\kappa)$ is characterized by one additional parameter only

$$f = \frac{P}{P_{\text{th}}} - 1, \quad (32)$$

that is the normalized excess pump intensity above the threshold value P_{th} (defined as the one corresponding to

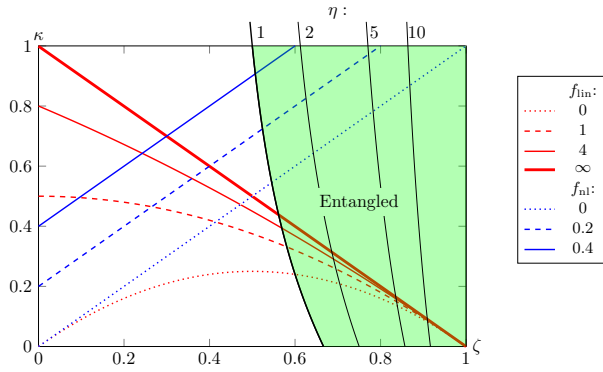


Figure 4: Phase diagram for polariton entanglement. The region of entanglement $\zeta > \zeta_{\text{crit}}^{\eta=1}(\kappa)$ is shaded in green and limited by the lines $\zeta_{\text{crit}}^{\eta}(\kappa)$ for $\eta > 1$ (the higher is the reservoir effective temperature T_R , the higher is η). Red lines correspond to the dependence $\kappa(\zeta)$ within the model (30), blue ones are the ones given by the model (31), f is the normalized excess pump intensity as defined by (32).

the vanishing condensate $\rho \rightarrow 0$). We derive the flux elasticity dependence (κ) on the entangled pumping intensity ζ :

$$\kappa(\zeta) = \frac{[1 - \zeta][\zeta + f]}{1 + f}$$

for the saturation model (30) and

$$\kappa(\zeta) = f + \zeta \quad (33)$$

for the linear saturation model (31). A series of curves is depicted in Figure 4 for both models showing the depen-

dence $\zeta(\kappa)$ for various values of f . Intersecting the proper curve with the boundary of entanglement corresponding to the value of η of the particular experimental setup (dependent, *e.g.*, on reservoir temperature, exciton-photon detuning, reservoir chemical potential) gives the minimal amount of entangled flux that is sufficient to reach an entangled stationary state. Note that the fact that the lines for the two models are significantly different at high values of ζ is due to the artificial nature of the linear saturation model, which technically allows for negative $P_{\text{lin}}[\rho]$, *i.e.* reversed coherent flow from the condensate to the reservoir.

We expect a real polaritonic system to lose stability ($\kappa < 0$) at a sufficiently high intensity of pumping with entangled pairs. More specifically, the equilibrium condition (14) suggests that for $2\chi > \Gamma[\rho_m]$ the pumping term $P[\rho_m]$ should be negative, which is not feasible in polaritonic systems. That is why we show only the region $\zeta \in [0; 1]$ in Figure 4. Note that $\zeta = 1$ is exactly the point where the model (30) predicts unstable density growth.

V. THE ENTANGLEMENT LIFETIME

Given that it is possible to reach an entangled state, we are interested in its lifetime. In this section, we will focus on the simplest linear saturation model with $P(\rho) = P_0 - \alpha\rho$ and a constant decay rate Γ , which allows for analytical solutions. We consider the following "driving protocol" for the condensates under consideration:

$$\chi(t) = \Theta(-t)\chi_0, \quad (34)$$

i.e., a sudden switching off. Using Ito's lemma, one may derive the following equations for $t > 0$ from (8)-(9) with $\chi = 0$ (see Appendix B and, *e.g.*, [21]):

$$d\rho_j = \left[(P_0 - \alpha\rho_j) \left(\rho_j + \frac{1}{2} \right) - \Gamma \left(\rho_j - \frac{1}{2} \right) \right] dt + \sqrt{(P_0 - \alpha\rho_j + \Gamma) \rho_j} \delta W_j(t), \quad (35)$$

$$d\theta_j = \sqrt{\frac{1}{4} \frac{P_0 - \alpha \langle \rho_j \rangle + \Gamma}{\langle \rho_i \rangle}} d\Omega_j \quad (36)$$

with independent Wiener increments dW_j and $d\Omega_j$. Here we also use the assumption $\langle \rho_j \rangle \gg \sqrt{\text{Var}(\rho_j)}$ and set η to unity (no backflow from the exciton reservoir) for simplicity. Tracing the evolution of the Wigner function in the weak-noise limit, where the Gaussian approximation is valid in terms of ρ_j and θ_+ , we may use the mean values $\rho_m(t) = \langle \rho_j \rangle(t)$ when calculating the noise variance and use Wick's/Iserliss's theorem to derive (see Appendix B

for details):

$$\begin{cases} d_t \rho_m &= (P_0 - \alpha\rho_m)\rho_m \\ d_t C &= 2(P_0 - 2\alpha\rho_m - \Gamma)C + (P_0 - \alpha\rho_m + \Gamma)\rho_m \\ d_t C_{12} &= 2(P_0 - 2\alpha\rho_m - \Gamma)C_{12}. \end{cases} \quad (37)$$

Here we assume that the means evolve independently, being "external" parameters for $C = \langle \delta\rho_j^2 \rangle(t)$ and $C_{12} = \langle \delta\rho_1 \delta\rho_2 \rangle(t)$. Under these approximations, it is straight-

forward to obtain an analytical solution. Specifically, if we use $\tau = \Gamma t$ as a time variable,

$$\rho_m(\tau) = \frac{f\Gamma}{\alpha} \frac{f + \zeta_0}{f + \zeta_0(1 - e^{-f\tau})} \quad (38)$$

and, thus, using Eq. (36),

$$C_\theta(\tau) = C_\theta(0) + \frac{1}{4} \int_0^\tau \left(\frac{f+2}{\rho_m(z)} - \frac{\alpha}{\Gamma} \right) dz. \quad (39)$$

Having the analytical expressions for means and variances (see Appendix B for complete expressions), one can trace the evolution of the squeezing degree $\xi(\tau)$ to see when it is below the threshold value $1 - 1/2\rho_m(\tau)$ as suggested by Eq. (24) (the structure of the covariance matrix does not change during evolution). This will define the entanglement lifetime τ_d , which characterizes the time interval $[0; \tau_d]$ during which the system is guaranteed to remain entangled. In the general case, one can find τ_d only numerically, although a simple analytical expression may serve as an upper bound for that time (being exact for $f(\zeta_0 - 0.4) \gg 1$, see Appendix C):

$$\tau_d(\zeta) = \frac{5}{2\zeta_0} \left[\zeta_0 - \frac{2}{5} \right], \quad (40)$$

which shows how the entanglement lifetime depends on the relative entangled pumping strength at $t < 0$. Comparing this expression with Eq. (38), one may see that the relaxation timescale for condensate density is $\sim [f\Gamma]^{-1}$ and for entanglement it is of the order of Γ^{-1} .

VI. DISCUSSION AND CONCLUSIONS

This work is intended to demonstrate the principal possibility to entangle two spatially separated polariton condensates despite their noisy evolution due to the coupling to the exciton reservoirs and the photon leakage. We believe that this result, along with the estimates for the necessary level of entangled particle flux, may serve as a guide for future experiments and as a reference point for assessing the feasibility of polariton-based quantum computing devices.

In addition, we have demonstrated that the initially entangled condensates do not live much longer than the photon lifetime in the cavity. The fundamental limit for the entanglement lifetime, which is critical for potential quantum computation applications of polaritons, is set by the photon lifetime, and, as one could intuitively expect, it should be increased to provide enough time for performing useful operations with entangled states.

However, there is an interesting feature inherent to the entanglement mechanism for the polaritonic condensates. Analysis of the expression (21) along with evolution equations (B2)-(B3) implies that after the entanglement pumping is turned off, the amplitude correlations relax at the scale of $\sim [f\Gamma]^{-1}$, the entanglement vanishes

at the scale of $\sim \Gamma^{-1}$, although the ratio $[C - C_{12}]/\rho_m^2$ remains small (as a consequence of the weak noise approximation for condensates above threshold). Importantly, the anisotropy relaxation time scale is mainly defined by the growth of C_θ . Given the factor of $1/\rho_m$ in the equation (39), the time estimate for C_θ to become of the order of unity is $\rho_m\Gamma^{-1}$, which is much longer (for typical experimental sample sizes and densities, condensate occupation ρ_m is of the order of $10^2 - 10^3$) than the density relaxation time. The entanglement criterion is much more demanding in terms of the degree of squeezing of the (x_j, p_{3-j}) distribution, as shown by the criterion (24). However, analyzing Eq. (21) along with expressions from Appendix C, one may see that the squeezing itself is present in the system for a much longer time than the entanglement. This might be useful for metrological applications of polaritonic condensates.

It is important to note that in the considered toy model two polariton condensates are assumed to be spatially separated and fully independent. No interactions between polaritons belonging to different condensates or excitons belonging to different reservoirs is taken into account. This regime may be of special importance for the realization of quantum repeaters based on exciton-polariton condensates. In contrast, quantum processors based on polariton qubits would necessarily rely on coupling of trapped polariton condensates, which may be done *e.g.* by recycling of photons emitted by one condensate to another condensate with the use of external mirrors [22]. Another important remark concerns the estimate of the entanglement life-time given in this work. In the recent experimental study of a qubit based on a trapped exciton-polariton condensate [23] the coherence times T1 and T2 of such a qubit have been found to exceed the single polariton life-time by at least two orders of magnitude (that is much longer than the entanglement life-time estimate given in our work). It would be very interesting to measure the coherence times of pairs of such qubits, especially, if they are initially driven to an entangled state (e.g. due to the resonant excitation by entangled photon pairs, as suggested in our work). Clearly, more theoretical and experimental research is needed to fully explore the rich quantum physics of many-body driven-dissipative bosonic condensates of exciton-polaritons.

-
- [1] Matteo Fadel, Tilman Zibold, Boris Décamps, and Philipp Treutlein. Spatial entanglement patterns and einstein-podolsky-rosen steering in bose-einstein condensates. *Science*, 360(6387):409–413, 2018.
- [2] Paolo Colciaghi, Yifan Li, Philipp Treutlein, and Tilman Zibold. Einstein-podolsky-rosen experiment with two bose-einstein condensates. *Phys. Rev. X*, 13:021031, May 2023.
- [3] Jingyan Feng, Ebubechukwu O. Ilo-Okeke, Alexey N. Pyrkov, Alexis Askitopoulos, and Tim Byrnes. Sensitive detection of entanglement in exciton-polariton condensates via spin squeezing. *Phys. Rev. A*, 104:013318, Jul 2021.
- [4] Jingyan Feng, Hui Li, Zheng Sun, and Tim Byrnes. Entanglement generation and detection in split exciton-polariton condensates. *Phys. Rev. A*, 108:053301, Nov 2023.
- [5] Álvaro Cuevas, Juan Camilo López Carreño, Blanca Silva, Milena De Giorgi, Daniel G. Suárez-Forero, Carlos Sánchez Muñoz, Antonio Fieramosca, Filippo Cardano, Lorenzo Marrucci, Vittorianna Tasco, Giorgio Bisasiol, Elena Del Valle, Lorenzo Dominici, Dario Ballardini, Giuseppe Gigli, Paolo Mataloni, Fabrice P. Laussy, Fabio Sciarrino, and Daniele Sanvitto. First observation of the quantized exciton-polariton field and effect of interactions on a single polariton. *Science Advances*, 4(4):eaa06814, April 2018.
- [6] Alexey Kavokin, Timothy C. H. Liew, Christian Schneider, Pavlos G. Lagoudakis, Sebastian Klembt, and Sven Hoeffling. Polariton condensates for classical and quantum computing. *Nature Reviews Physics*, 4(7):435–451, July 2022.
- [7] Sanjib Ghosh and Timothy C. H. Liew. Quantum computing with exciton-polariton condensates. *npj Quantum Information*, 6(1):16, February 2020.
- [8] Yan Xue, Igor Chestnov, Evgeny Sedov, Evgeniy Kiktenko, Aleksey K. Fedorov, Stefan Schumacher, Xuekai Ma, and Alexey Kavokin. Split-ring polariton condensates as macroscopic two-level quantum systems. *Phys. Rev. Res.*, 3:013099, Jan 2021.
- [9] Marcello Calvanese Strinati and Claudio Conti. Quantum hyperspins: Highly nonclassical collective behavior in quantum-optical parametric oscillators. *Phys. Rev. A*, 111:043712, Apr 2025.
- [10] B. R. Mollow and R. J. Glauber. Quantum theory of parametric amplification. i. *Phys. Rev.*, 160:1076–1096, Aug 1967.
- [11] B. R. Mollow and R. J. Glauber. Quantum theory of parametric amplification. ii. *Phys. Rev.*, 160:1097–1108, Aug 1967.
- [12] Michiel Wouters and Vincenzo Savona. Stochastic classical field model for polariton condensates. *Phys. Rev. B*, 79:165302, Apr 2009.
- [13] H. Haug, T. D. Doan, and D. B. Tran Thoai. Quantum kinetic derivation of the nonequilibrium gross-pitaevskii equation for nonresonant excitation of microcavity polaritons. *Phys. Rev. B*, 89:155302, Apr 2014.
- [14] A. A. Elistratov and Yu. E. Lozovik. Polariton bose condensate in an open system: Ab initio approach. *Phys. Rev. B*, 97:014525, Jan 2018.
- [15] Crispin W. Gardiner. *Handbook of Stochastic Methods*, volume 13 of *Springer Series in Synergetics*. Springer Berlin Heidelberg, Berlin, Heidelberg, 1983. Chapter 5, section 5.3, pages 163-165.
- [16] C W. Gardiner and P. Zoller. *Quantum noise: a handbook of Markovian and non-Markovian quantum stochastic methods with applications to quantum optics*. Springer complexity. Springer, third edition. edition. OCLC: 903068139.
- [17] H. T. C. Stoof. Coherent versus incoherent dynamics during bose-einstein condensation in atomic gases. *Journal of Low Temperature Physics*, 114(1):11–108, Jan 1999. 63-64.
- [18] Alessia Allevi, Maria Bondani, Paulina Marian, Tudor A. Marian, and Stefano Olivares. Characterization of phase-averaged coherent states. *J. Opt. Soc. Am. B*, 30(10):2621–2627, Oct 2013.
- [19] R. Simon. Peres-horodecki separability criterion for continuous variable systems. *Phys. Rev. Lett.*, 84:2726–2729, Mar 2000.
- [20] Jonathan Keeling and Natalia G. Berloff. Spontaneous rotating vortex lattices in a pumped decaying condensate. *Phys. Rev. Lett.*, 100:250401, Jun 2008.
- [21] Crispin W. Gardiner. *Handbook of Stochastic Methods*, volume 13 of *Springer Series in Synergetics*. Springer Berlin Heidelberg, Berlin, Heidelberg, 1983. Chapter 4, section 4.4, pages 107-109.
- [22] Joris Barrat, Andreas F Tzortzakakis, Meng Niu, Xiaoqing Zhou, Giannis G Paschos, David Petrosyan, and Pavlos G Savvidis. Qubit analog with polariton superfluid in an annular trap. *Sci Adv*, 10(43):eado4042, October 2024.
- [23] Roman V. Cherbunin, Aleksey Liubomirov, Stella V. Kavokina, Denis Novokreschenov, Andrey Kudlis, and Alexey V. Kavokin. Quantum beats of a macroscopic polariton condensate in real space. *Optics*, 6(4), 2025.

Appendices

Appendix A: Covariance matrix

In this appendix, we evaluate the covariance matrix elements, using the Gaussian approximation in ρ_1 , ρ_2 and θ_+ . We start from $\langle x_1^2 \rangle$ and take advantage of the

fact that the marginal angular distribution:

$$\begin{aligned} \langle x_1^2 \rangle &= \langle \rho_1 \cos^2(\theta_1) \rangle = \langle (\rho_m + \delta\rho_1) \rangle \langle \cos^2(\theta_1) \rangle \\ &= \frac{1}{2} (\rho_m + \langle \delta\rho_1 \rangle) = \frac{\rho_m}{2}. \end{aligned} \quad (\text{A1})$$

Similar arguments lead to $\langle x_{1/2}^2 \rangle = \langle p_{1/2}^2 \rangle = \rho_m^2/2$.

Clearly, $\langle x_1 p_1 \rangle = \langle x_2 p_2 \rangle = 0$ since $\langle \sin(\theta_{1/2}) \cos(\theta_{1/2}) \rangle = 0$. Next, using $\theta_1 = \pi/2 - (\theta_1 - \delta\theta)$:

$$\begin{aligned} \langle x_1 x_2 \rangle &= \langle \sqrt{\rho_1 \rho_2} \cos(\theta_1) \cos(\theta_2) \rangle = \left\langle \rho_m \left(1 + \frac{\delta\rho_2 + \delta\rho_1}{2\rho_m} + \frac{\delta\rho_1 \delta\rho_2}{2\rho_m} - \frac{1}{8} \left(\frac{\delta\rho_2 + \delta\rho_1}{\rho_m} \right)^2 \right) \cos(\theta_2) \sin(\theta_2 - \delta\theta) \right\rangle = \\ &= \left\langle \rho_m \left(1 - \frac{\delta\rho_2^2 + 2\delta\rho_2 \delta\rho_1 + \delta\rho_1^2}{8\rho_m^2} \right) \cos(\theta_2) \sin(\theta_2) \left[1 - \frac{\delta\theta^2}{2} \right] \right\rangle = 0. \end{aligned} \quad (\text{A2})$$

In the same fashion $\langle p_1 p_2 \rangle = 0$. The crucial non-zero terms are $\langle x_1 p_2 \rangle = \langle x_2 p_1 \rangle$. They are evaluated as follows:

$$\begin{aligned} \langle x_2 p_1 \rangle &= \langle \sqrt{\rho_1 \rho_2} \sin(\theta_1) \cos(\theta_2) \rangle = \left\langle \rho_m \left(1 + \frac{\delta\rho_2 + \delta\rho_1}{2\rho_m} + \frac{\delta\rho_1 \delta\rho_2}{2\rho_m} - \frac{1}{8} \left(\frac{\delta\rho_2 + \delta\rho_1}{\rho_m} \right)^2 \right) \cos(\theta_2) \cos(\theta_2 - \delta\theta) \right\rangle = \\ &= \left\langle \rho_m \left(1 - \frac{\delta\rho_2^2 - 2\delta\rho_2 \delta\rho_1 + \delta\rho_1^2}{8\rho_m^2} \right) \cos^2(\theta_2) \left[1 - \frac{\delta\theta^2}{2} \right] \right\rangle = \frac{1}{2} \rho_m \left\langle \left(1 - \frac{\delta\rho_2^2 - 2\delta\rho_2 \delta\rho_1 + \delta\rho_1^2}{8\rho_m^2} \right) \left[1 - \frac{\delta\theta^2}{2} \right] \right\rangle = \\ &= \frac{\rho_m}{2} \left\langle 1 - \frac{\delta\rho_2^2 - 2\delta\rho_2 \delta\rho_1 + \delta\rho_1^2}{8\rho_m^2} - \frac{\delta\theta^2}{2} + \frac{\delta\rho_2^2 - 2\delta\rho_2 \delta\rho_1 + \delta\rho_1^2}{8\rho_m^2} \frac{\delta\theta^2}{2} \right\rangle = \frac{\rho_m}{2} \left[1 - \frac{\langle \delta\rho_{2/1}^2 \rangle - \langle \delta\rho_2 \delta\rho_1 \rangle}{4\rho_m^2} - \frac{\langle \delta\theta^2 \rangle}{2} \right]. \end{aligned} \quad (\text{A3})$$

Given that all the first order quadrature averages are zero, these expressions justify the structure of the covariance matrix presented in the main text. In addition to these calculations, it is instructive to express the variances in rotated quadratures, which are used in the main text, *e.g.* $q_{\pm} = \frac{x_1 \pm p_2}{\sqrt{2}}$:

$$\begin{aligned} \langle q_{\pm}^2 \rangle &= \frac{\langle x_1^2 \rangle + \langle p_2^2 \rangle}{2} \pm \langle x_1 p_2 \rangle \\ &= \frac{\rho_m}{2} \left[1 \pm 1 \mp \left(\frac{\langle \delta\rho_2 \delta\rho_1 \rangle}{4\rho_m^2} + \frac{\langle \delta\theta^2 \rangle}{2} \right) \right]. \end{aligned} \quad (\text{A4})$$

Appendix B: Evolution equations for the means and cumulants

In this Appendix, we provide derivations of the results of Section V. We start from equations (8) assuming

the constant decay rate Γ , the linear pumping saturation model (31), $\chi = 0$, and $\eta = 1$:

$$\begin{cases} dx_j = \frac{1}{2} [(P_0 - \alpha\rho_j - \Gamma)x_j] dt + \sqrt{\frac{1}{4}(P_0 - \alpha\langle\rho_j\rangle + \Gamma)} dW_{x_j}, \\ dp_j = \frac{1}{2} [(P_0 - \alpha\rho_j - \Gamma)p_j] dt + \sqrt{\frac{1}{4}(P_0 - \alpha\langle\rho_j\rangle + \Gamma)} dW_{p_j}. \end{cases} \quad (\text{B1})$$

We then invert the Madelung transformation $\rho_j = x_j^2 + p_j^2$, $\theta_j = \arctan(p_j/x_j)$ and use Ito's lemma to derive the following equations after Madelung transformation:

$$d\rho_j = 2x_j dx_j + 2p_j dp_j + (dx_j)^2 + (dp_j)^2 = \left[(P_0 - \alpha\rho_j) \left(\rho_j + \frac{1}{2} \right) - \Gamma \left(\rho_j - \frac{1}{2} \right) \right] dt + \sqrt{(P_0 - \alpha\rho_j + \Gamma) \rho_j} \delta W_j(t), \quad (\text{B2})$$

$$d\theta_j = \frac{\partial\theta_j}{\partial x_j} dx_j + \frac{\partial\theta_j}{\partial p_j} dp_j + \frac{1}{2} \left(\frac{\partial^2\theta_j}{\partial x_j^2} (dx_j)^2 + 2 \frac{\partial^2\theta_j}{\partial x_j \partial p_j} dx_j dp_j + \frac{\partial^2\theta_j}{\partial p_j^2} (dp_j)^2 \right) = \sqrt{\frac{1}{4} \frac{P_0 - \alpha\langle\rho_j\rangle + \Gamma}{\langle\rho_i\rangle}} d\Omega_j(t). \quad (\text{B3})$$

Here we introduce two independent Wiener increments:

$$\begin{pmatrix} dW_j \\ d\Omega_j \end{pmatrix} = \begin{pmatrix} \cos \theta_j & \sin \theta_j \\ -\sin \theta_j & \cos \theta_j \end{pmatrix} \begin{pmatrix} dW_{xj} \\ dW_{pj} \end{pmatrix} \quad (\text{B4})$$

The rate equations for the mean values are obviously given by:

$$d_t \langle \rho_j \rangle = \left(P_0 - \Gamma - \frac{\alpha}{2} \right) \langle \rho_j \rangle - \alpha \langle \rho_j \rangle^2 - \alpha C_j \quad (\text{B5})$$

For the higher moments we use the Ito's lemma twice more:

$$\begin{aligned} d_t C_j &= \frac{2 \langle \rho_j d\rho_j \rangle + \langle d\rho_j^2 \rangle - 2 \langle \rho_j \rangle d \langle \rho_j \rangle}{dt} = 2 \left\langle \left[(P_0 - \alpha \rho_j) \left(\rho_j + \frac{1}{2} \right) - \Gamma \left(\rho_j - \frac{1}{2} \right) \right] \rho_j \right\rangle + \langle (P_0 - \alpha \rho_j + \Gamma) \rho_j \rangle \\ &\quad - 2 \left\langle \left[(P_0 - \alpha \rho_j) \left(\rho_j + \frac{1}{2} \right) - \Gamma \left(\rho_j - \frac{1}{2} \right) \right] \right\rangle \langle \rho_j \rangle = (2P_0 - \alpha - 2\Gamma) C_j + (P_0 + \Gamma) \langle \rho_j \rangle - 2\alpha \langle \rho_j^3 \rangle + 2\alpha (C_j + \langle \rho_j \rangle^2) \langle \rho_j \rangle, \\ d_t C_{12} &= \frac{d \langle \rho_1 \rho_2 \rangle - d(\langle \rho_1 \rangle \langle \rho_2 \rangle)}{dt} = \left\langle \left[(P_0 - \alpha \rho_1) \left(\rho_1 + \frac{1}{2} \right) - \Gamma \left(\rho_1 - \frac{1}{2} \right) \right] \rho_2 + \left[(P_0 - \alpha \rho_2) \left(\rho_2 + \frac{1}{2} \right) - \Gamma \left(\rho_2 - \frac{1}{2} \right) \right] \rho_1 \right\rangle \\ &\quad - \left\langle \left[(P_0 - \alpha \rho_1) \left(\rho_1 + \frac{1}{2} \right) - \Gamma \left(\rho_1 - \frac{1}{2} \right) \right] \right\rangle \langle \rho_2 \rangle + \left\langle \left[(P_0 - \alpha \rho_2) \left(\rho_2 + \frac{1}{2} \right) - \Gamma \left(\rho_2 - \frac{1}{2} \right) \right] \right\rangle \langle \rho_1 \rangle = \\ &= (2P_0 - 2\Gamma) C_{12} - \alpha \langle \rho_2^2 \rho_1 + \rho_1^2 \rho_2 \rangle + \alpha (\langle \rho_2^2 \rangle \langle \rho_1 \rangle + \langle \rho_1^2 \rangle \langle \rho_2 \rangle). \end{aligned} \quad (\text{B6})$$

Isserlis' theorem allows for further simplification with the help of the following identities:

$$\begin{aligned} \langle \rho_j^3 \rangle &= \langle \rho_j \rangle^3 + 3 \langle \rho_j \rangle C_j \\ \langle \rho_2^2 \rho_1 + \rho_1^2 \rho_2 \rangle - \langle \rho_2^2 \rangle \langle \rho_1 \rangle - \langle \rho_1^2 \rangle \langle \rho_2 \rangle &= 2(\langle \rho_1 \rangle + \langle \rho_2 \rangle) C_{12}. \end{aligned}$$

Thus,

$$d_t C_j = (2P_0 - \alpha - 2\Gamma) C_j + (P_0 + \Gamma) \langle \rho_j \rangle \quad (\text{B7})$$

$$\begin{aligned} &\quad - 2\alpha (\langle \rho_j \rangle^3 + 3 \langle \rho_j \rangle C_j) + 2\alpha (C_j + \langle \rho_j \rangle^2) \langle \rho_j \rangle \\ d_t C_{12} &= (2P_0 - 2\Gamma) C_{12} - 2\alpha (\langle \rho_1 \rangle + \langle \rho_2 \rangle) C_{12} \end{aligned} \quad (\text{B8})$$

in the scope of the weak-noise approximation $\langle \rho_j \rangle^2 \gg C_{1/2/12}$ the equations for the means decouple from the others:

$$d_t \langle \rho_j \rangle = (P_0 - \alpha \langle \rho_j \rangle - \Gamma) \langle \rho_j \rangle \quad (\text{B9})$$

and may be solved explicitly and expressed in terms of the dimensionless time $\tau = \Gamma t$, parameters $\zeta_0 = 2\chi/\Gamma$ and $f = P/P_{\text{th}} = P_0/\Gamma$ from the main text:

$$\langle \rho_1 \rangle(\tau) = \langle \rho_2 \rangle(\tau) = \rho_m(\tau) = \frac{f\Gamma}{\alpha} \frac{f + \zeta_0}{f + \zeta_0(1 - e^{-f\tau})}. \quad (\text{B10})$$

Here we took advantage of the symmetry of the initial distribution (10) and used (14) to define the initial conditions.

Within the same weak-noise approximation, the equations for cumulants read as follows ($C(\tau) = C_1(\tau) = C_2(\tau)$ due to the symmetry of the equations and the initial distribution):

$$d_\tau C = 2 \left(f - 2 \frac{\alpha \rho_m}{\Gamma} \right) C + \left(f - \frac{\alpha \rho_m}{\Gamma} \right) \rho_m, \quad (\text{B11})$$

$$d_\tau C_{12} = 2 \left(f - 2 \frac{\alpha \rho_m}{\Gamma} \right) C_{12}. \quad (\text{B12})$$

Considering $\rho_m(t)$ as an external parameter, we obtain explicitly:

$$C(t) = \left[\frac{f}{f + \zeta_0(1 - e^{-f\tau})} \right]^4 C(0) e^{-2f\tau} + \frac{\Gamma}{\alpha} e(t), \quad (\text{B13})$$

$$C_{12}(t) = \left[\frac{f}{f + \zeta_0(1 - e^{-f\tau})} \right]^4 C_{12}(0) e^{-2f\tau} \quad (\text{B14})$$

with $e(\tau)$ interpolating between $e(0) = 0$ and $e(\infty) = 1$:

$$e(\tau) = \left[\frac{f + \zeta_0}{f + \zeta_0(1 - e^{-f\tau})} \right]^4 \left[(1 - e^{-f\tau}) \left[1 - \frac{f(\zeta_0 - 1) + 5\zeta_0}{f + \zeta_0} e^{-f\tau} - \frac{(f + 2)\zeta_0^3}{(f + \zeta_0)^3} e^{-2f\tau} \right] + \frac{2\zeta_0^2 f (f + 3) e^{-2f\tau}}{(f + \zeta_0)^2} \right]. \quad (\text{B15})$$

Finally, we derive the equation for the angular variation.

Since the evolution equation (B3) describes pure diffu-

sion, it is straightforward:

$$dC_\theta = \frac{1}{4} \frac{\Gamma(f+2) - \alpha\rho_m(\tau)}{\Gamma\rho_m(\tau)} d\tau, \quad (\text{B16})$$

thus:

$$\begin{aligned} C_\theta &= C_\theta(0) + \frac{1}{4} \int_0^\tau \left(\frac{f+2}{\rho_m(z)} - \frac{\alpha}{\Gamma} \right) dz \\ &= C_\theta(0) + \frac{\alpha}{\Gamma} \left[-\frac{(f+2)\zeta_0(1-e^{-f\tau})}{4f^2(f+\zeta_0)} + \frac{\tau}{2f} \right]. \end{aligned} \quad (\text{B17})$$

Appendix C: The estimation of disentanglement time

The initial value of the squeezing parameter for the linear saturation model is given by

$$\begin{aligned} \xi_0 &= 1 - \frac{1}{4\rho_m^2} \frac{(2\Gamma-2\chi)(\alpha\rho_m)}{2\alpha(\alpha\rho_m+2\chi)} - \frac{2\Gamma-2\chi}{16\chi\rho_m} = \\ &= 1 - \frac{1}{4} \frac{2-\zeta_0}{2\rho_m\left(\frac{\alpha\rho_m}{\Gamma} + \zeta_0\right)} - \frac{2-\zeta_0}{8\zeta_0\rho_m} = \\ &= 1 - \frac{2-\zeta_0}{8\rho_m} \left[\frac{1}{f+2\zeta_0} + \frac{1}{\zeta_0} \right]. \end{aligned} \quad (\text{C1})$$

Here we substituted $\eta = 1$, $\rho_m = (P_0 - \Gamma + 2\chi)/\alpha$, $G'[\rho_m] = \alpha$. The initial state is entangled if the inequality (24) is satisfied, which leads to:

$$\zeta_0 = \frac{1}{22} \left[6 - 5f + \sqrt{36 + 28f + 25f^2} \right]. \quad (\text{C2})$$

One may check that this is the same result as one would obtain by solving equations (28) and (31).

Analyzing the solutions (B10), (B13), (B14) and (B17), we see that the radial correlations decay exponentially, while the angular one grows only linearly at large times:

$$C_\theta(\tau \rightarrow \infty) = \frac{\alpha}{\Gamma} \left[\underbrace{\frac{2-\zeta_0}{4\zeta_0(f+\zeta_0)}}_{\text{initial value}} - \frac{(f+2)\zeta_0}{4f^2(f+\zeta_0)} + \frac{1}{2f}\tau \right]. \quad (\text{C3})$$

So, at a late time $\tau \gg \frac{1}{f}$, when all the radial correlations have already faded out, the squeezing degree is given by the following expression:

$$\xi(\tau) = 1 - \frac{C(\infty)}{4\rho_m^2(\infty)} - \frac{C_\theta(\tau \rightarrow \infty)}{2} = \quad (\text{C4})$$

$$= 1 - \frac{\alpha}{\Gamma} \left[\frac{1}{4f^2} + \frac{(2-\zeta_0)f - 2\zeta_0}{8f^2\zeta_0} + \frac{1}{2f}\tau \right]. \quad (\text{C5})$$

Once the radial distribution has already relaxed towards the new equilibrium, the entanglement threshold is given by

$$\zeta_{\text{cr}} = 1 - \frac{1}{2\rho_m(\infty)} = 1 - \frac{\alpha}{\Gamma} \frac{1}{2f}, \quad (\text{C6})$$

thus, the entanglement criterion is as follows:

$$\left[\frac{1}{4f^2} + \frac{(2-\zeta_0)f - 2\zeta_0}{8f^2\zeta_0} + \frac{1}{4f}\tau \right] < \frac{1}{2f}. \quad (\text{C7})$$

It is satisfied while $\tau < \tau_d$ with the disentanglement time given by

$$\tau_d = \frac{5}{2} - \frac{1}{\zeta_0}. \quad (\text{C8})$$

Since $\zeta_0 = 0.4$ is the minimum critical value required to achieve entanglement (see Eq. (28)), this expression is always positive. It is a good approximation if at the time of disentanglement τ_d the radial distribution has already relaxed to the new equilibrium, which is the case if $f\tau_d \gg 1$ or, taking advantage of $\zeta \in [0.4; 1]$,

$$f \left(\zeta_0 - \frac{2}{5} \right) \gg 1. \quad (\text{C9})$$

Outside of this parameter region, the expression (C8) is only an upper bound for the value of the critical time. We have verified it numerically, using exact solutions (B10), (B13), (B14) and (B17).